IOP Publishing Journal of Physics D: Applied Physics

J. Phys. D: Appl. Phys. **53** (2020) 124002 (9pp) https://doi.org/10.1088/1361-6463/ab634d

Antimicrobial effects and mechanism of plasma activated fine droplets produced from arc discharge plasma on planktonic *Listeria monocytogenes* and *Escherichia coli* O157:H7

K H Baek[1], H I Yong[2], J H Yoo[1], J W Kim[1], Y S Byeon[3], J Lim[3], S Y Yoon[3], S Ryu[3] and C Jo[1]

[1] Department of Agricultural Biotechnology, Center for Food and Bioconvergence, and Research Institute of Agriculture and Life Science, Seoul National University, Seoul 08826, Republic of Korea
[2] Research Group of Food Processing, Korea Food Research Institute, Wanju 55365, Republic of Korea
[3] Plasma Technology Research Center of National Fusion Research Institute, 37, Dongjangsan-ro, Gunsan-si, Jeollabuk-do, 54004, Republic of Korea

E-mail: cheorun@snu.ac.kr

Received 16 August 2019, revised 14 November 2019
Accepted for publication 18 December 2019
Published 13 January 2020

Abstract

In this study, we investigated the antimicrobial effects of plasma activated fine droplet (PAD) produced from arc discharge plasma on planktonic *Listeria monocytogenes* and *Escherichia coli* O157:H7. NaCl (0.9%, w/v) was used as the feeding solution for the plasma discharge. The inactivation mechanism of the PAD treatment was also investigated. PAD mainly contains H_2O_2 and OCl^-, which play a significant role in the inactivation process against *L. monocytogenes* and *E. coli* O157:H7. The population of *L. monocytogenes* and *E. coli* O157:H7 was significantly reduced by approximately 3 and 4 log units, respectively, within 5 min of exposure to PAD. However, the bactericidal effects of PAD against *L. monocytogenes* and *E. coli* O157:H7 showed different trends by showing 0.58 and 4.13 log reductions, respectively, after 1 min of PAD exposure time. The change of membrane integrity was evaluated using two DNA-binding fluorescence dyes, SYTO 9 and propidium iodide (PI). The breakage of the cell wall and membrane of both microorganisms was evidenced by the uptake of PI by cells after 5 min of exposure to PAD, but the effect was less in *L. monocytogenes* compared to *E. coli* O157:H7 after 1 min of PAD exposure time. The transmission electron microscopy results clearly showed morphological changes in both microorganisms, including denaturation or leakage of intracellular materials as a consequence of PAD treatment. These findings suggest that PAD-induced chemical species can eventually affect the intracellular materials of bacterial cells by passing through or attacking the cell envelope. In addition, *L. monocytogenes* are less susceptible to PAD compared with *E. coli* O157:H7.

Keywords: arc discharge plasma, plasma activated fine droplet, *Listeria monocytogenes*, *Escherichia coli* O157:H7, microbial inactivation mechanism

S Supplementary material for this article is available online

(Some figures may appear in colour only in the online journal)

 © 2020 IOP Publishing Ltd Printed in the UK

1. Introduction

In recent years, with the increasing consumption of various food products, foodborne outbreaks have been constantly reported [1–3]. These outbreaks can occur from every step of production through farms, post harvesting, transportation, slaughtering, storage, distribution, and finally consumption. In practice, contaminated livestock transport vehicles can be sources of various disease pathogens, infecting other abattoirs and animals [4]. Furthermore, cross-contamination can occur when the food comes into contact with contaminated equipment during the production process [5]. Thus, the amount and occurrence of pathogens varies depending on the management of the food distribution channel, and it is especially important to control *Listeria monocytogenes* and *Escherichia coli* O157:H7, which are major foodborne pathogens that can potentially lead to foodborne infections [6].

L. monocytogenes, a Gram-positive bacterium, is a pathogenic agent causing listeriosis; the disease can be fatal to humans and has a high mortality rate of 20%–40% [7]. One of the characteristics of *L. monocytogenes* is that it can adapt to refrigerated environments and can even form biofilms, which is a concern for the contemporary food industry, particularly in slaughterhouses [8]. *E. coli* O157:H7, a Gram-negative bacterium, can mainly cause bloody diarrhea and hemolytic-uremic syndrome occasionally [9], and there is a significant risk of contamination of meat from livestock animals by *E. coli* O157:H7 [6]. Despite technological advances, foodborne disease outbreaks by these pathogens have continuously occurred, requiring efficient pasteurization techniques to effectively control the growth of microorganisms in various environments.

Plasma, especially atmospheric pressure plasma (APP), has attracted attention as a non-thermal pasteurization technology [10, 11]. Because of the presence of primary and secondary species, plasma possess bactericidal [12], fungicidal [13, 14], and viricidal [15] effects. However, plasma technology has spatial limitations because it is difficult to apply to environments where plasma is difficult to access, such as deep inside pipes and areas of equipment or devices [5]. To overcome these limitations and to apply plasma to a wide area, research has recently been conducted on applying plasma to water, which is called plasma-treated water [16–18].

Recently, plasma-treated water has gained increasing attention as an environment friendly and cost-effective aqueous disinfectant [19]. Because some plasma-induced chemical species can dissolve or penetrate into water to produce primary and secondary species [20], plasma-treated water exhibits antibacterial and anti-biofilm activities [21, 22]. It is generally agreed that the existence of reactive species such as ·OH, H_2O_2, O_3, NO_2^-, and NO_3^- may contribute to the antibacterial activity of plasma-treated water [20, 23], and plasma-treated water is known to be effective even when applied in different ways, such as a spray [24] or mist [25, 26]. Therefore, plasma-treated water has the potential to be applied to various environments because it can overcome spatial limitations of other approaches. Therefore, studies on the antibacterial effects for various uses of plasma-treated water should be carried out, and optimal pasteurization conditions for new applications should be established.

In this study, we produced plasma-activated droplet (PAD), a type of plasma-treated water, as an aqueous disinfectant using arc discharge plasma without any gas injection. The aim of this study was to clarify the antimicrobial effects and the mechanisms of PAD on planktonic *L. monocytogenes* and *E. coli* O157:H7, which are representative Gram-positive and -negative foodborne pathogens, respectively.

2. Experimental setups and methods

2.1. Plasma source and preparation of PAD

Figure 1 and table 1 show a schematic diagram of the experimental apparatus and conditions used in this study. Plasma discharge was generated between cylindrical tungsten and titanium electrodes separated by ceramic plates. Electric power for plasma generation was provided by an alternating current (AC) power supply (IPS-1500, Insung Heavy Industry Co., Ltd, Busan, Korea). The electrical discharge was formed in electrically conductive liquid without additional gas injection, and the PAD was spurted through a hole (2 mm) (figure S1 (stacks.iop.org/JPhysD/53/124002/mmedia)). A petri dish was used to collect PAD for 10 s, and the distance between the end of the hole and the petri dish was 15 cm. Distilled water containing NaCl (0.9% w/v) was used as the feeding solution to provide conductive characteristics of liquid for the plasma discharge. Current and voltage profiles during the plasma discharge were acquired by a current probe (Model 110, Pearson Electronics, Inc., Palo Alto, CA, USA) and a voltage probe (P6015A, Tektronix, Beaverton, OR, USA), respectively, using a digital oscilloscope (DPO 2024, Tektronix, Beaverton, OR, USA).

2.2. Chemical measurements in PAD

The chemical properties of PAD produced from different liquid flow rates (40, 50, 60, and 70 ml min^{-1}) were determined immediately, including temperature, pH, electric conductivity, and the concentrations of hydrogen peroxide (H_2O_2), free available chlorine (FAC; HOCl or OCl^-), nitrate anions (NO_3^-), and nitrite anion (NO_2^-). Temperature was measured using a digital thermometer (YF-160 Type-K, YFE, Hsinchu City, Taiwan), and the pH value was measured using a pH meter (SevenGo, Mettler-Toledo International Inc., Schwerzenbach, Switzerland). The electric conductivity was measured using an Orion conductivity meter (VSTAR52, Thermo Scientific, Waltham, MA, USA) equipped with a conductivity probe (Orion 013005MD, Thermo Scientific, USA). H_2O_2 was analyzed based on a previous method [21] with slight modifications by using ammonium metavanadate (99%; Sigma-Aldrich GmbH, Steinheim, Germany). The reaction is based on a red-orange color change caused by peroxovanadium cation, which is formed by the reaction between H_2O_2 and metavanadate under acidic conditions. To measure the H_2O_2 concentration in PAD, one milliliter of the 10 mM ammonium metavanadate and 0.3 ml of 5 M sulfuric acid (95%; Junsei Chemical

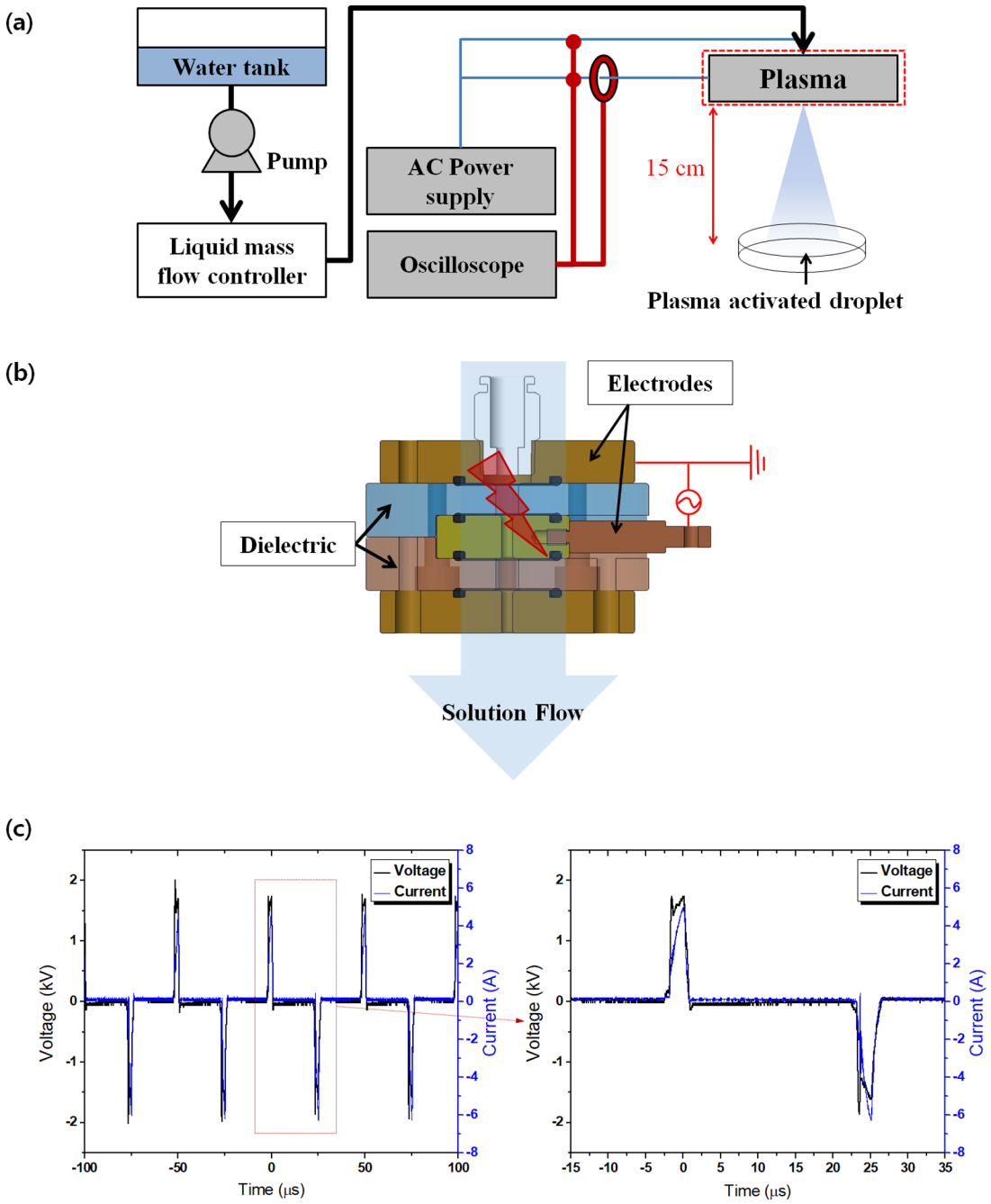

Figure 1. Schematic diagram showing the generation of plasma activated droplet (a) produced from arc discharge (b) and current and voltage profile during discharge (c).

Co. Ltd, Chuo-ku, Japan) were added to 1 ml of PAD. After 2 min, the absorbance was measured at 450 nm by using a UV/Vis spectrophotometer (X-ma 3100, Human Co. Ltd, Seoul, Korea). A standard curve was used to calculate the concentration of H_2O_2 in samples. The concentration of FAC was analyzed using the colorimetric method based on the N,N-diethyl-p-phenylenediamine (DPD) chemistry using a free chlorine assay kit (HS-Cl_2, Humas, Daejeon, Korea). The concentration of NO_2^- was analyzed by measuring nitrite-nitrogen (NO_2-N) using test kits (TNT840, HACH Co., Loveland, CO, USA), and the concentration of NO_3^- was analyzed by measuring the nitrate-nitrogen (NO_3-N) using the HACH Test 'N Tube Reactor/Cuvette Tubes with NItraVer X Reagent (Chromotropic Acid method). A spectrophotometer (DR 1900, HACH Co., Loveland, CO, USA) was used for absorbance measurements to analyze FAC, NO_3^-, and NO_2^-.

2.3. Bacterial strain and culture conditions

The Gram-positive bacterium *L. monocytogenes* (ATCC 19111) and Gram-negative bacterium *E. coli* O157:H7 (NCCP 15739) for this study were provided by the Korean Culture Center of Microorganisms (Seoul, Korea) and the National Culture Collection for Pathogen (Osong, Korea), respectively. *L. monocytogenes* was cultivated in fresh sterile tryptic soy broth (TSB; Difco, Becton Dickinson Co., Sparks, MD, USA) containing

Table 1. Conditions of arc discharge.

Parameter	Conditions
Peak voltage	2 kV
Peak current	1.5 A
Frequency	20 kHz
Pulse width	3 μs
Feeding solution	0.9% w/v NaCl
Solution flow rate	40–70 ml min^{-1}
Hole diameter	2 mm
Dielectric composition	Ceramic
Powered electrode composition	Tungsten
Ground electrode composition	Titanium

Table 2. Temperature, pH, and electric conductivity of PAD.

Liquid flow rate (ml min^{-1})	Temperature (°C)	pH	Conductivity (mS cm^{-1})
Before discharge	20.9[e]	6.52[c]	15.8[f]
40	47.1[d]	8.26[b]	18.1[b]
50	49.5[c,d]	8.13[b]	17.6[c]
60	50.5[c]	8.08[b]	17.4[d]
70	53.1[b]	8.15[b]	17.1[e]
SEM[a]	0.513	0.080	0.032

[a] Standard error of the mean ($n = 15$).
[b–f] Different letters within the same column differ significantly ($P < 0.05$).

0.6% yeast extract, and *E. coli* O157:H7 was cultivated in fresh sterile TSB (Difco) medium. They were incubated at 37 °C and 120 rpm orbital agitation for 24 h. The cells were harvested by centrifugation at 2265 g for 15 min at 4 °C in a refrigerated centrifuge (UNION 32R, Hanil Science Industrial, Co., Ltd Korea) and washed twice with sterile 0.85% saline solution. The final pellets were resuspended in 0.85% saline solution, corresponding to approximately 10^8 to 10^9 CFU ml^{-1}.

2.4. Analysis of the antibacterial ability of PAD

A volume of 4.5 ml of PAD or sterile 0.85% saline solution was transferred into sterile 50 ml tubes containing 0.5 ml of each bacterial suspension. The volume ratio of PAD and bacterial suspension in this study was consistent with other research using plasma treated water or electrolyzed water [27, 28]. The obtained bacterial suspensions were mixed thoroughly for 5 s and incubated at room temperature for different time intervals (1, 2, 3, 4, and 5 min). Following each incubation, tenfold serial dilutions of the 100 μl bacterial suspension were plated onto agar plates and incubated at 37 °C for 24 h. The medium used for *L. monocytogenes* was tryptic soy agar (TSA; Difco, Becton Dickinson Co., Sparks, MD, USA) containing 0.6% yeast extract, and the medium used for *E. coli* O157:H7 was TSA (Difco). All colonies were counted, and the number of microorganisms was expressed as log CFU/ml.

2.5. Determination of cell membrane integrity

A BacLight™ Live/Dead Bacterial viability kit (L-7012; Molecular Probes, Eugene, OR, USA) was used to evaluate cell membrane integrity. The kit contains two DNA-binding dyes, SYTO 9 (green fluorescence) and propidium iodide (PI, red fluorescence). Green fluorescence indicates membrane intact bacteria, whereas red fluorescence of PI indicates membrane damaged bacteria. Therefore, PAD-induced cellular membrane disruption could be successfully evaluated.

After PAD treatment (0, 1, and 5 min), the planktonic bacteria in suspension were immediately separated from PAD after centrifugation at 13 200 g for 2 min (HM-150IV, Hanil Co., Ltd., Incheon, Korea) and resuspended in 0.1 M phosphate-buffered saline (PBS, pH 7.4). The dye mixture (3 μl) was dripped into 1 ml of the PAD-treated bacterial suspension and incubated for 20 min at room temperature in the darkness. Each sample (5 μl) was then dripped onto a slide glass (Paul Marienfeld GmbH & Co. KG, Laud-Königshofen, Germany) which had a thickness of 1 mm and covered for examination on a confocal laser scanning microscope (Leica TCS SP8 X, Wetzlar, Germany) using appropriate filters with excitation/emission wavelengths at 483/490–540 nm for SYTO 9 and excitation/emission wavelengths at 535/590–680 nm for PI.

2.6. Transmission electron microscopy

To evaluate the morphological changes in *L. monocytogenes* and *E. coli* O157:H7 resulting from PAD treatment, transmission electron microscopy (TEM) analysis was performed. The planktonic bacteria in suspension were immediately separated from PAD and resuspended in 0.1 M PBS (pH 7.4). The cell pellets were collected by centrifugation at 8000 g for 10 min and fixed at 4 °C for 2 h in modified Karnovsky's fixative, consisting of 2% paraformaldehyde and 2% glutaraldehyde in 0.05 M sodium cacodylate buffer (pH 7.2). After primary fixation, each sample was washed three times with 0.05 M sodium cacodylate buffer at 4 °C for 10 min and postfixed in 1% osmium tetroxide in 0.05 M sodium cacodylate buffer at 4 °C for 2 h. The fixed sample was rinsed twice with distilled water and stained with 0.5% uranyl acetate at 4 °C for 24 h. The stained sample was dehydrated at room temperature with a graded ethanol series (15 min each) of 30, 50, 70, 80, and 90% and finally repeated thrice at 100%. Transition was performed twice with 100% propylene oxide for 15 min each, and then, the sample was infiltrated with a 1:1 solution of 100% propylene oxide and Spurr's resin for 2 h. The sample was immersed into Spurr's resin for 24 h and then re-immersed in Spurr's resin for 2 h for the final infiltration. The sample was polymerized at 70 °C for 24 h and sectioned using an ultramicrotome (MT-X, RMC, Tucson, AZ, USA) before TEM analysis. The microstructure of each bacterial cell was observed using a transmission electron microscope (JEM-1010, JEOL, Tokyo, Japan) at 80 kV.

2.7. Statistical analysis

Each experiment was performed in triplicate. The data were analyzed using SAS statistical software program (version 9.4, SAS Institute Inc., Cary, NC, USA). Statistical analysis was performed by one-way analysis of variance (ANOVA),

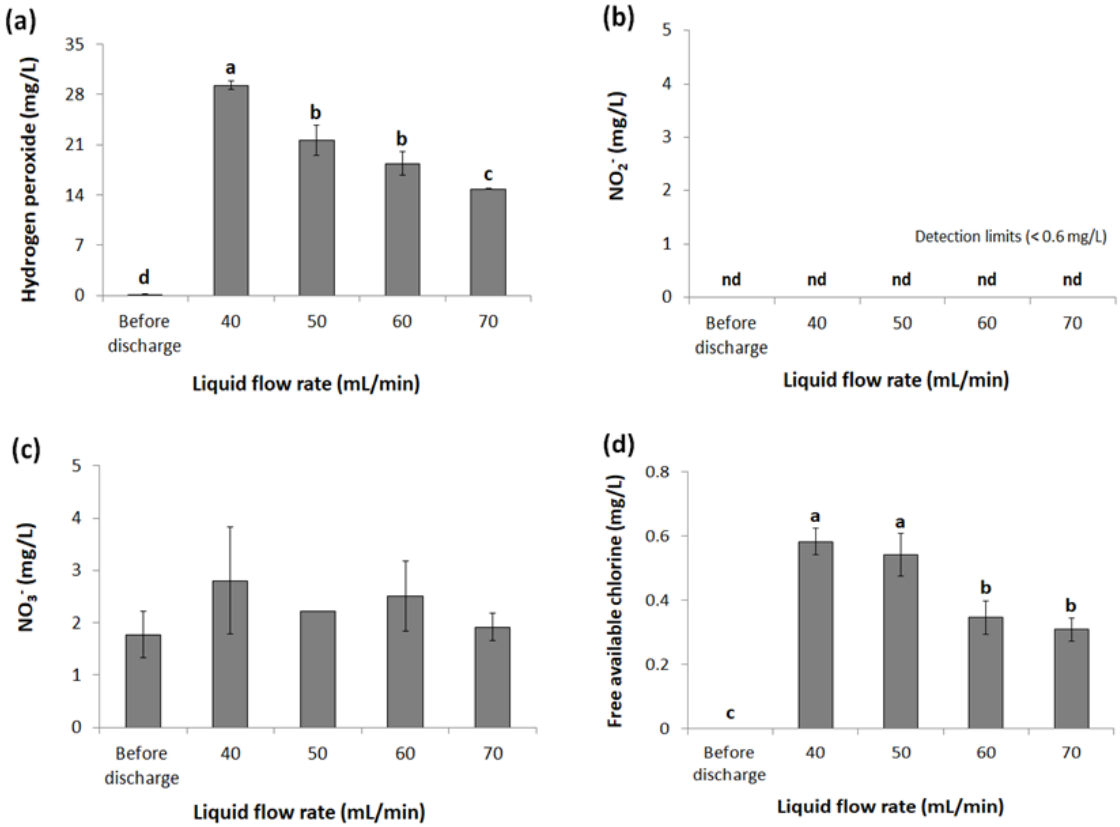

Figure 2. Hydrogen peroxide (a), nitrite (b), nitrate (c), and free available chlorine (d) concentration of PAD according to the liquid flow rate (0, 40, 50, 60, and 70 ml min^{-1}). Error bars denote standard deviation. [a–d] Different letters differ significantly ($P < 0.05$).

with a completely randomized design, using the general linear model. Significant differences among the mean values were determined using the Tukey's multiple comparison test at a significance level of $P < 0.05$.

3. Results and discussion

3.1. Chemical characterization of plasma

Table 2 shows the temperature, pH, and electric conductivity of the untreated solution (0.9% w/v NaCl) and PAD produced from different liquid flow rates (40, 50, 60, and 70 ml min^{-1}).

The temperature of PAD was 47.1 °C at 40 ml min^{-1} of liquid flow rate, and it increased in proportion with the liquid flow rate. This is attributed to the accumulation of high temperature PAD as the liquid flow rate is increased. The pH of the PAD increased from 6.52 before discharge to 8.08–8.26, and no difference was observed depending on the liquid flow rate. Kondeti *et al* [29] reported a large pH increase in saline solution by applying APP jet with air in Ar or 1% O_2, and Jirásek & Lukeš [30] suggested that plasma-induced pH increase in saline solution is due to the alkaline characteristics of hypochlorite ions (OCl^-) and its capturing of hydrogen ions (H^+) (see equation (13)). In our previous studies [31, 32], the pH of the plasma treated water dramatically decreased during plasma treatment. In the case of atmospheric air discharge, nitrogen oxides (such as NO, NO_2, and N_2O_3) are mainly produced and react with water molecules, resulting in the formation of HNO_2 and HNO_3 [21]. These molecules release hydrogen ions through deprotonation reactions, thus acidifying water. However, air was not injected for plasma discharge in the present system; therefore, the generation of reactive nitrogen species (RNS) can be negligible. The increase in electric conductivity was the largest up to 18.1 mS cm^{-1} at 40 ml min^{-1} of liquid flow rate possibly because of the formation of chemical species, but the electric conductivity decreased with increasing liquid flow rate by the dilution effect.

Figure 2 shows the concentrations of H_2O_2, NO_2^-, NO_3^-, and FAC in the untreated solution (0.9% w/v NaCl) and PAD produced from different liquid flow rates (40, 50, 60, and 70 ml min^{-1}). Here, we considered H_2O_2 as an indicator of ROS formation because it is stable with a relatively long lifetime, up to 10 h (at pH 7.0) in aqueous environments [33] and it can be dissociated into hydroxyl radicals (·OH), which are the strongest oxidants [34] but are difficult to detect because of their short lifetime [33]. In figure 2(a), the highest concentration of H_2O_2, 29.3 mg l^{-1}, was found at the lowest liquid flow rate (40 ml min^{-1}), which was consistent with our observation of the highest electric conductivity at 40 ml min^{-1} of liquid flow rate. Burlica *et al* [35] also found the same trends for the formation of H_2O_2 from water spray produced by pulsed gliding arc plasma with different carrier gases and water flow rates.

In plasma generated in the confined area between the electrodes, a higher increase in ·OH and ·H can occur because of

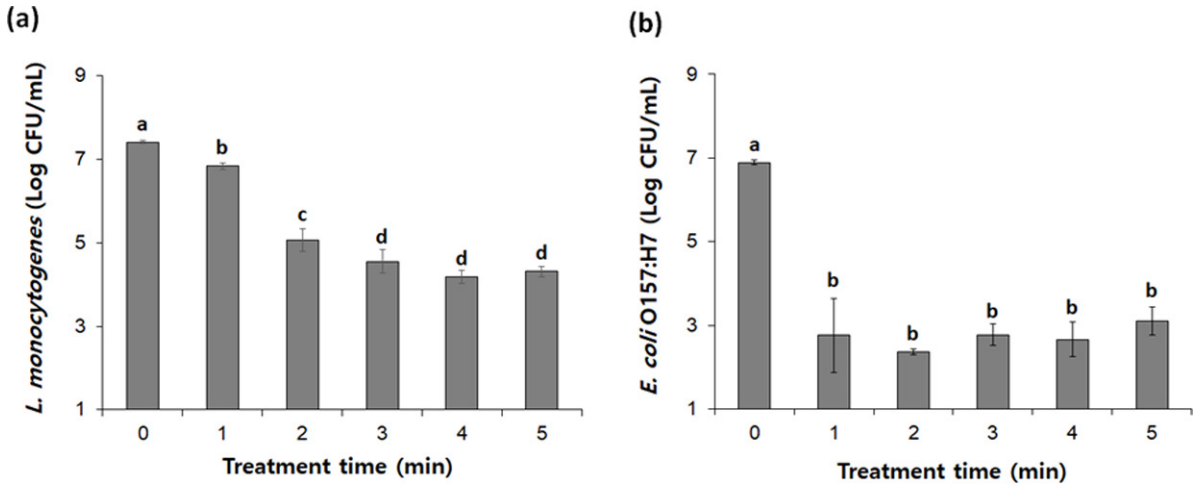

Figure 3. Surviving population (log CFU ml^{-1}) of *L. monocytogenes* (a) and *E. coli* O157:H7 (b) after being exposed to the PAD (0, 1, 2, 3, 4, and 5 min). Error bars denote standard deviation. [a–d] Different letters differ significantly ($P < 0.05$).

the high temperature thermal dissociation of water caused by the collision of water molecules in the confined spaces. This reaction can be given by the following equation [36].

$$H_2O + M \rightarrow \cdot OH + \cdot H + M \quad (1)$$

where $M = H_2O$.

Moreover, direct water dissociation may occur according to equations (2) and (3), and both H_2O_2 and H_2 may be formed through an overall reaction (4), including possible ·OH recombination and other pathways [35].

$$H_2O + e^- \rightarrow H + \cdot OH + 2e- \quad (2)$$

$$H_2O + e^- \rightarrow 2H + O + e- \quad (3)$$

$$2H_2O \rightarrow H_2O_2 + H_2. \quad (4)$$

H_2O_2 can be dissociated to ·OH by reactions (5)–(9) [5, 34].

$$H_2O_2 \rightarrow \cdot OH + \cdot OH \quad (5)$$

$$H_2O_2 + \cdot H \rightarrow H_2O + \cdot OH \quad (6)$$

$$H_2O_2 + \cdot O \rightarrow HO_2 + \cdot OH \quad (7)$$

$$H_2O_2 + e^- \rightarrow \cdot OH + OH^- \quad (8)$$

$$H_2O_2 + \cdot HO_2 \rightarrow H_2O + O_2 + \cdot OH. \quad (9)$$

As shown in figures 2(b) and (c), the concentration of NO_2^- in PAD was lower than the minimum detection limit (0.6 mg l^{-1}) for all treatment groups, and there was no significant difference in NO_3^- content. Because air was not injected for plasma discharge in this system, the generation of reactive nitrogen species (RNS) can be assumed to be negligible, which shows similar trends with the previous study using underwater capillary discharge system [24].

The plasma discharge showed the formation of FAC in the PAD, and the concentrations of FAC were 0.58 and 0.54 mg l^{-1} at liquid flow rates of 40 and 50 ml min^{-1}, respectively (figure 2(d)). We expected that hypochlorous acid (HOCl) and hypochlorite ion (OCl^-) could be produced by reactions (10)–(13) when the saline solution was exposed to plasma as follows [37].

$$H_2O \leftrightarrow H^+ + \cdot OH + e^- \quad (10)$$

$$Cl^- \leftrightarrow \cdot Cl + e^- \quad (11)$$

$$Cl + \cdot OH \leftrightarrow HOCl \quad (12)$$

$$HOCl \leftrightarrow H^+ + OCl^-. \quad (13)$$

Because OCl^- is more stable in alkaline water [30, 38], the major component of FAC in our system could be OCl^-. The antimicrobial effects of OCl^- are relatively poorer than those of HOCl, but it can also exert an oxidizing action from outside of the cell [39]. As mentioned before, ROS with a lifetime in the order of nanoseconds can exist in the PAD, resulting in microbial inactivation. However, measuring of the short-lived ROS in the PAD is difficult and beyond the scope of the present research. In this regard, we considered that long-lived ROS, short-lived ROS that may have been generated, and FAC mainly composed of OCl^- were significantly responsible for the bactericidal effects in the current system. For measuring the bactericidal activities of PAD, a liquid flow rate of 40 ml min^{-1} was chosen for the optimal condition corresponding to the highest H_2O_2 and FAC formation (figure 2).

3.2. Bacterial viable count

The inactivation patterns of PAD-treated *L. monocytogenes* and *E. coli* O157:H7 cells are depicted in figure 3. The surviving population of *L. monocytogenes* significantly reduced by 0.58 log CFU ml^{-1} after 1 min of exposure to PAD and further decreased in proportion to the treatment time (figure 3(a)). As a result, the surviving population of *L. monocytogenes* significantly reduced by 3.10 log CFU ml^{-1} after 5 min of exposure to PAD. However, *E. coli* O157:H7 inactivation required a shorter treatment time compared to that needed to inactivate *L. monocytogenes*. The surviving population of *E. coli* O157:H7 significantly reduced by 4.13 log CFU ml^{-1} after 1 min of treatment time (figure 3(b)), but no additional

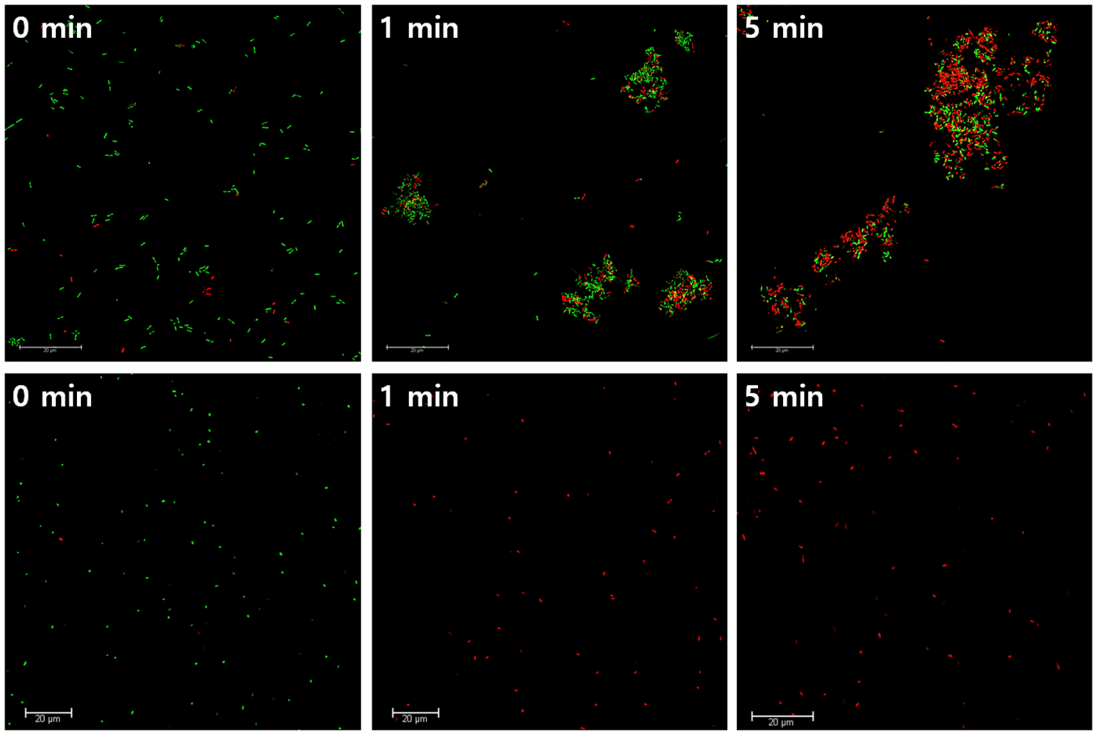

Figure 4. Fluorescence images of bacterial cells without or with PAD treatment. *L. monocytogenes* (upper) and *E. coli* O157:H7 (bottom) after 0, 1, and 5 min of exposure to PAD, respectively.

antimicrobial effects were observed as the treatment time increased. There was no more significant reduction observed in both pathogens after 5 min of treatment (figure S2). These data indicate that PAD has antimicrobial effects against both *L. monocytogenes* and *E. coli* O157:H7 cells and are especially more potent for *E. coli* O157:H7, which is a Gram-negative bacterium. Several studies have shown the different antimicrobial effects of plasma treatment against Gram-positive and Gram-negative bacteria [19, 40]. The relative ineffectiveness of PAD against Gram-positive bacteria can be explained by the relatively dense peptidoglycan structures, leading to less PAD sensitivity. Gram-positive bacteria have a thick (20–80 nm) cell wall as the outer shell of the cell [41]. In contrast, Gram-negative bacteria have a relatively thin peptidoglycan layer (<10 nm) of cell wall and an outer membrane consisting of lipopolysaccharides and phospholipids [42]. Our results show that the Gram-negative *E. coli* O157:H7 with a thin cell wall had a significant higher susceptibility to PAD treatment compared with Gram-positive *L. monocytogenes* with a thick cell wall. As Gram-positive bacteria are less susceptible to chemical oxidation [1, 23], more active exposure is required from aqueous ROS to break down the thick cell wall of *L. monocytogenes*.

3.3. Membrane integrity

The fluorescence images of the counterstained PAD-treated planktonic *L. monocytogenes* and *E. coli* O157:H7 are depicted in figure 4. SYTO 9 can penetrate the intact cell membrane of bacteria, thus staining all bacteria to green, while PI can penetrate only membrane-damaged bacteria, resulting in a reduction of SYTO 9 stain fluorescence [43]. The untreated cells of both bacterial species mostly have intact cell membranes, and the membrane permeability of *L. monocytogenes* was slightly increased when exposed to 1 min of PAD. More cells were stained with PI when exposed to 5 min of PAD compared with 1 min PAD-treated cells. However, the membrane permeability of *E. coli* O157:H7 to PI increased dramatically after only 1 min exposure to PAD. These results supported the fact that *E. coli* O157:H7 could be more effectively inactivated than *L. monocytogenes* by PAD-induced membrane damages. According to Xu *et al* [23] who compared the plasma-driven antimicrobial effects against to *Staphylococcus aureus* (NCTC-8325) and *E. coli* (ATCC-25922), more *E. coli* cells lost their membrane integrity than *S. aureus* cells, suggesting the susceptibility difference between Gram-positive and Gram-negative bacteria to plasma. In our results, formation of pores in the membrane of *L. monocytogenes* and *E. coli* O157:H7 was evidenced by uptake of PI by cells after 5 min of exposure to PAD.

3.4. Morphological analysis

PAD-induced morphological changes of *L. monocytogenes* and *E. coli* O157:H7 were examined by TEM (figure 5). The untreated cells of both bacterial species showed intact cell membranes. In *L. monocytogenes* cells treated with PAD for 1 min, the outer shell was slightly damaged, and deformation of intracellular materials was observed. However, when *L. monocytogenes* cells were exposed to PAD for 5 min, obvious morphological changes were observed, including leakage of intracellular materials and breakage of cell wall. In the case of

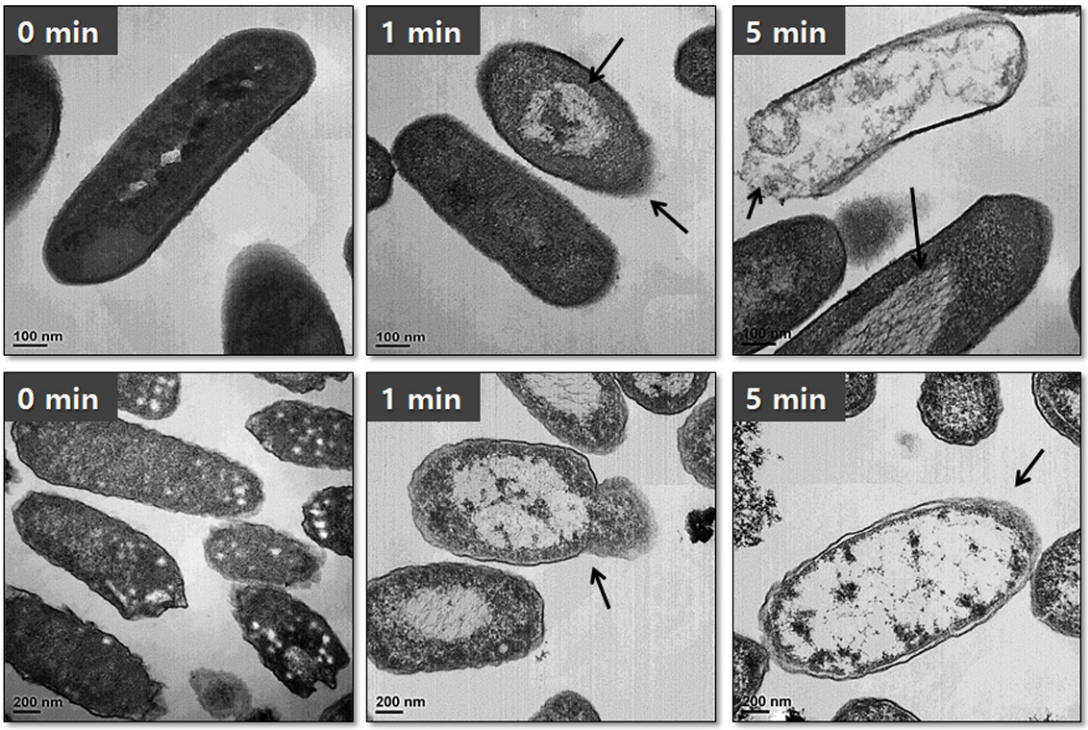

Figure 5. TEM images of bacterial cells without or with PAD treatment. *L. monocytogenes* (upper) and *E. coli* O157:H7 (bottom) after 0, 1, and 5 min of exposure to PAD, respectively. The deformation and efflux of intracellular materials of membrane-damaged cells were observed (black arrows).

E. coli O157:H7, dramatic structural changes were observed only 1 min after exposure to PAD. These results also suggest, as previously discussed, that *E. coli* O157:H7 was more susceptible to PAD than *L. monocytogenes*, and the outer cell structure of both bacterial species can be damaged by PAD-induced chemical attacks, which results in cell damage or cell death. Ji *et al* [19] suggest that reactive species produced from the plasma can eventually damage the intracellular DNA and RNA by attacking the chemical bonds of the cell membrane, which are mainly composed of proteins, fatty acids, lipids, and phospholipids. Moreover, the bactericidal action of plasma can be possibly explained by diffusion, in which reactive species can pass through the cell membrane and attack intracellular nucleic acids and proteins, leading to cell death [44].

4. Conclusion

PAD produced from arc discharge plasma mainly contains H_2O_2 as ROS and OCl^-, which play a significant role in the inactivation process against both *L. monocytogenes* and *E. coli* O157:H7 cells. PAD reduced the number of both pathogenic bacteria, but *L. monocytogenes* was less susceptible to PAD than *E. coli* O157:H7 possibly because of the different outer structures of the cells. Nevertheless, PAD treatment can disrupt both the outer cell walls and membranes of *L. monocytogenes* and *E. coli* O157:H7, which is accompanied by the denaturation or leakage of intracellular nucleic acids and proteins. These findings suggest that PAD-induced chemical species can eventually affect the intracellular materials of bacterial cells by passing through or attacking the cell envelope.

Acknowledgments

This work was supported by the R&D Program of 'Plasma Advanced Technology for Agriculture and Food (Plasma Farming)' through the National Fusion Research Institute of Korea (NFRI) funded by government funds. Also, this work was supported by the BK21 Plus Program of the Department of Agricultural Biotechnology, Seoul National University, Seoul, Korea.

ORCID iDs

K H Baek https://orcid.org/0000-0002-5438-9547
H I Yong https://orcid.org/0000-0003-0970-4496
J H Yoo https://orcid.org/0000-0003-1057-8036
J W Kim https://orcid.org/0000-0001-8934-4771
Y S Byeon https://orcid.org/0000-0003-2153-9534
J Lim https://orcid.org/0000-0001-9249-9360
S Y Yoon https://orcid.org/0000-0003-0118-8474
S Ryu https://orcid.org/0000-0002-0001-2963
C Jo https://orcid.org/0000-0003-2109-3798

References

[1] Yong H I, Kim H J, Park S, Kim K, Choe W, Yoo S J and Jo C 2015 *Food Res. Int.* **69** 57–63
[2] Seo J, Seo D J, Oh H, Jeon S B, Oh M H and Choi C 2016 *Food Sci. Anim. Resour.* **36** 186–93
[3] Karyotis D, Skandamis P N and Juneja V K 2017 *Food Res Int.* **100** 894–8
[4] Ni L, Zheng W, Zhang Q, Cao W and Li B 2016 *Prev. Vet. Med.* **133** 42–51

[5] An J Y, Yong H I, Kim H J, Park J Y, Lee S H, Baek K H, Choe W and Jo C 2019 *Appl. Phys. Lett.* **114** 073703
[6] Huang L, Hwang C A and Fang T 2019 *Food Control.* **96** 29–38
[7] Alsheikh A D I, Mohammed G E, Abdalla M A and Bakhiet A O 2014 *Br. Microbiol. Res. J.* **4** 28–38
[8] Oliveira T S, Varjão L M, da Silva L N N, Pereira R D C L, Hofer E, Vallim D C and de Castro Almeida R C 2018 *Food Control* **88** 131–8
[9] Abuladze T, Li M, Menetrez M Y, Dean T, Senecal A and Sulakvelidze A 2008 *Appl. Environ. Microbiol.* **74** 6230–8
[10] Misra N N and Jo C 2017 *Trends Food Sci. Tech.* **64** 74–86
[11] Yong H I, Lee S H, Kim S Y, Park S, Park J, Choe W and Jo C 2019 *Innov. Food Sci. Emerg.* **53** 78–84
[12] Gavahian M, Chu Y H and Jo C 2019 *Compr. Rev. Food Sci. Food Saf.* **18** 1292–309
[13] Yong H I, Lee H, Park J, Choe W, Jung S and Jo C 2017 *Meat Sci.* **123** 151–6
[14] Misra N N, Yadav B, Roopesh M S and Jo C 2019 *Compr. Rev. Food Sci. Food Saf.* **18** 106–20
[15] Puligundla P and Mok C 2016 *Res. J. Biotechnol.* **11** 91–6
[16] Yong H I, Park J, Kim H J, Jung S, Park S, Lee H J, Choe W and Jo C 2018 *Plasma Porcess Polym.* **15** e1700050
[17] Hozák P, Scholtz V, Khun J, Mertová D, Vaňková E and Julák J 2018 *Plasma Phys. Rep.* **44** 799–804
[18] Machala Z, Tarabová B, Sersenová D, Janda M and Hensel K 2019 *J. Phys. D: Appl. Phys.* **52** 034002
[19] Ji S H, Ki S H, Ahn J H, Shin J H, Hong E J, Kim Y J and Choi E H 2018 *Arch. Biochem. Biophys.* **643** 32–41
[20] Shen J, Tian Y, Li Y, Ma R, Zhang Q, Zhang J and Fang J 2016 *Sci. Rep.* **6** 28505
[21] Park J Y, Park S, Choe W, Yong H I, Jo C and Kim K 2017 *ACS Appl. Mater. Interfaces* **9** 43470–7
[22] Wu S, Zhang Q, Ma R, Yu S, Wang K, Zhang J and Fang J 2017 *Eur. Phys. J. Spec. Top.* **226** 2887–99
[23] Xu Z, Cheng C, Shen J, Lan Y, Hu S, Han W and Chu P K 2018 *Bioelectrochemistry* **121** 125–34
[24] Hong Y C, Huh J Y, Ma S H and Kim K I 2018 *J. Electrost.* **91** 56–60
[25] Bingyan C, Changping Z, Juntao F, Xiang H, Cheng Y, Yuan W, Yongfeng J, Longwei C, Yuan G and Qingbang H 2016 *Plasma Sci. Technol.* **18** 41–50
[26] Ranieri P, McGovern G, Tse H, Fulmer A, Kovalenko M, Nirenberg G, Miller V, Fridman A, Rabinovich A and Fridman G 2018 *IEEE Trans. Plasma Sci.* **47** 395–402
[27] Xiang Q, Kang C, Niu L, Zhao D, Li K and Bai Y 2018 *LWT-Food Sci. Technol.* **96** 395–401
[28] Abadias M, Usall J, Oliveira M, Alegre I and Viñas I 2008 *Int. J. Food Microbiol.* **123** 151–8
[29] Kondeti V S S K, Phan C Q, Wende K, Jablonowski H, Gangal U, Granick J L, Hunter R C and Bruggeman P J 2018 *Free Radic. Biol. Med.* **124** 275–87
[30] Jirásek V and Lukeš P 2019 *Plasma Sources Sci. Technol.* **28** 035015
[31] Jung S, Kim H J, Park S, Yong H I, Choe J H, Jeon H J, Choe W and Jo C 2015 *Food Sci. Anim. Resour.* **35** 703–6
[32] Yong H I, Han M, Kim H J, Suh J Y and Jo C 2018 *Sci. Rep.* **8** 9790
[33] Burns J M *et al* 2012 *Aquat. Sci.* **74** 683–734
[34] Shang K, Li J, Wang X, Yao D, Lu N, Jiang N and Wu Y 2016 *Japan. J. Appl. Phys.* **55** 01AB02
[35] Burlica R, Shih K Y and Locke B R 2010 *Ind. Eng. Chem. Res.* **49** 6342–9
[36] Mededovic S and Locke B R 2007 *J. Phys. D: Appl. Phys.* **42** 049801
[37] Lee S J, Ma S-H, Hong Y C and Choi M C 2018 *Sep. Purif. Technol.* **193** 351–7
[38] Kim H W and Chung N Y 2012 *J. Korean Soc. Manuf. Technol. Eng.* **21** 720–5
[39] Fukuzaki S 2006 *Biocontrol Sci.* **11** 147–57
[40] Han L, Patil S, Boehm D, Milosavljević V, Cullen P J and Bourke P 2016 *Appl. Environ. Microbiol.* **82** 450–8
[41] Mai-Prochnow A, Clauson M, Hong J and Murphy A B 2016 *Sci. Rep.* **6** 38610
[42] Amro N A, Kotra L P, Wadu-Mesthrige K, Bulychev A, Mobashery S and Liu G Y 2000 *Langmuir* **16** 2789–96
[43] Stiefel P, Schmidt-Emrich S, Maniura-Weber K and Qun R 2015 *BMC Microbiol.* **15** 36
[44] Ziuzina D, Patil S, Cullen P J, Keener K M and Bourke P 2013 *J. Appl. Microbiol.* **114** 778–87